

An Efficient and Integrated Approach for the Detection of Blood Vessels and Exudates in Color Fundus Images

S. Sankaranarayanan, M. Anto Bennet, G. Vijayalakshmi, N. Sathya and T.R. Dinesh kumar

Department of Electronics and Communication Engineering,
VELTECH Avadi-Chennai-600062, Tamilnadu, India

Abstract: Diabetic-related eye disease is a major cause of preventable blindness in the world. It is a complication of diabetes which can also affect various parts of the body. When the small blood vessels have a high level of glucose in the retina, the vision will be blurred and can cause blindness eventually. This is known as diabetic retinopathy. Regular screening is essential in order to detect the early stages of diabetic retinopathy for timely treatment to prevent or delay further deterioration. This paper detects the presences of abnormalities in the retina such as the structure of blood vessels, micro aneurysms, exudates and texture properties using image processing techniques. These features are input into artificial neural network for automatic detection and can quickly process a large number of fundus images obtained from mass screening to help reduce the cost and increase productivity and efficiency for ophthalmologists.

Key words: Exudates • Diabetic Retinopathy (DR) • Fundus Image • Circular Fitting • Mathematical Morphology

INTRODUCTION

Diabetic retinopathy is a complication of diabetes and is a major cause of blindness in developed countries is shown in fig 1. It is estimated to account for 12% of all the new cases of blindness in United States annually. In Singapore, retinal disease accounts for more than half of the newly registered blindness with diabetic retinopathy as one of the main contributors. It is estimated that about 10% of the population over the age of 40 are affected with diabetes and about 20% of this group will develop some form of diabetic complications in the eye shown in fig 2. With the number rising every year, Singapore is one of the countries with the highest rate of diabetes in the world.

As a diabetic tends to have a lot of other health complications, going blind can have his problems multiplied. He will have problems in moving around and even in taking his medications. The patients might not notice a loss of vision until it became too severe, hence early diagnosis and timely treatment is vital to delay or prevent visual impair and even blindness.

Currently, regular screenings are conducted and retinal images are obtained using fundus camera is shown in fig 3 and its cross section shown in fig 4. However, a large amount of images are obtained from these screenings and it requires trained ophthalmologists to spend a lot of time for manual analysis and diagnosis. Hence, automatic detection is desired as it can help to improve productivity and be more cost effective.

Diabetic retinopathy occurs when the blood vessels of the retina in the posterior part of the eye are damaged. Damages due to small vessels would be known as micro vascular disease while damages due to the arteries would be macro vascular disease. PDR is the advanced stage whereby signals are sent by the retina to the body for the lack of blood supply and this triggered the growth of new blood vessels. These blood vessels can grow along the retina and the surface of the jelly-like substance (vitreous gel) which fills the centre of the eye. Although they are fragile and abnormal, they do not cause symptoms or vision loss. It is only when their thin and weak walls leak blood, severe visual loss or even irreversible blindness would occur shown in fig 5.



Fig. 1: .Normal Vision



Fig. 2: Vision of a person with diabetic retinopathy



Fig. 3: Example of a fundus camera

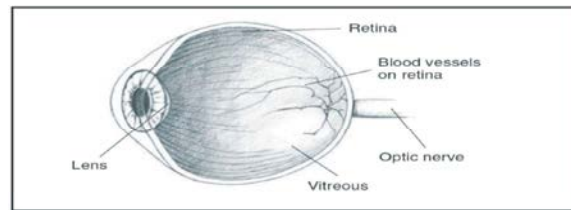


Fig. 4: Cross sectional view of the human eye

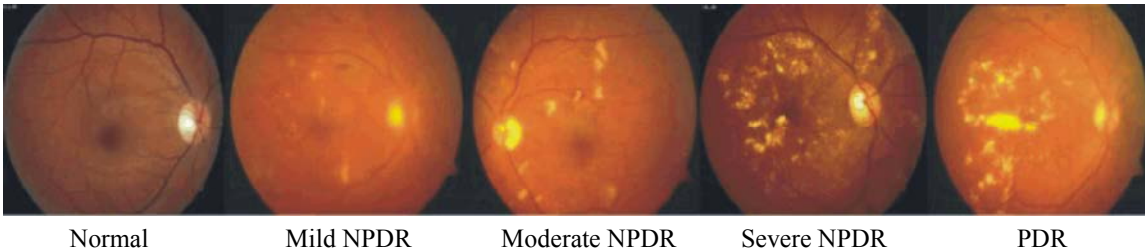


Fig. 5: Retinal fundus images of different stages of diabetic retinopathy

Existing System: The fundamental problem with glaucoma therapy today is that it treats the main risk factor as eye pressure without addressing the underlying reason for vision loss, which is damage to the retinal ganglion cells. Several researchers researched over the cause and treatment for the glaucoma and many methods for the early detection of the glaucoma have been evaluated and proposed leading to the maximum sensitivity and specificity for the detection. [1] investigated the value of fractal dimension in separating normal and cancerous by a “leave-one-out” analysis approach to classify the samples into group with sensitivity of 95% and specificity of 93% is obtained in this approach. [2] suggested a method for recognizing retina layers on Optical Coherence Tomography (OCT)

image by the classifiers SVM and Multi-Layer Perceptron (MLP). 98.6% accuracy for SVM and 96.6% accuracy for MLP neural network was reported. It shows the texture analysis as the ability to provide a mean for diagnosing differentiation of tissue. [3] presented a method with strong evidence that the fractal dimension of the blood vessels in the normal human retina is approximately 1.7. This is the same fractal dimension that was found for a diffusion limited growth process. [4] measures the cup to disc ratio based on line profile analysis in retinal images for early detection of glaucoma. Here blue channel of the color fundus image is used as it has higher contrast between the cup and regions. Zero crossing method is used to find cup edge. According to Autofocus algorithm algorithm, on an

average 95% limits of agreement between readers and the AF algorithm were -2.56 to 2.93 and -3.7 to 3.84 diopter respectively.

Jian Li *et al.* [5] proposed an efficient box-counting based method for the improvement of the fractal dimension estimation accuracy. This model is to assign the smallest no of boxes to cover the entire image surface at each selected scale as required, thereby yielding more accurate estimates. It has accuracy of 91.67% and sensitivity and specificity of 90% and 93.33% respectively. [6] proposed a novel automated glaucoma diagnosis using HOS cumulants extracted from radon transform applied on digital fundus images. The proposed system detected average accuracy of 84.72% using Naive Bayes classifier. [7] used different processing techniques for detection and classification of glaucoma. The different techniques are combined also to get the best method. Out of which Back Propagation algorithm has been considered as the better classifier. [8] described a novel low cost automated glaucoma diagnosis system based on hybrid feature extraction from digital fundus images. Furthermore they proposed a novel integrated index called Glaucoma Risk Index which is composed from Higher Order Spectra and Trace Transform features to diagnose the unknown class using a single feature. It has accuracy of 91.67% and sensitivity and specificity of 90% and 93.33% respectively.

Radim Kolar and JiriJan [9] proposed a method to detect glaucomatous eye based on fractal description by the classification. Fractal dimensions can be used as features for retinal nerve fibers loss detection of glaucoma. Performance was done by single box counting method and spectral based methods. 93% accuracy was achieved in this method.

Rajendra Aeharya *et al.* [10] quotes a method a novel method for glaucoma detection using a combination of texture and Higher Order Spectra features from digital fundus images and achieved 91% accuracy. SVM, Sequential Minimal Optimization, Naive Bayesian and Random Forest classifiers are used to perform supervised classification. [11] proposed automated glaucoma detection system that operates on inexpensive digital color fundus images. On the sample set of 575 fundus images a classification accuracy of 80% has been achieved in a 5 fold cross validation set. [12] described a novel diagnostic scheme to develop quantitative indexes of diabetes. The degree of lacunarity is reduced from the gap size distribution. The Back Propagation Algorithm,

Radial Basis Function Network, the Genetic Algorithm and the voting scheme are used. [13] proposed a method to detect the retinal morphological changes around the optical disc using multifractal approach. It was found that the vascular network geometry in patients with peripapillary atrophy has a multifractal geometry characterized of exponents. It has accuracy of 91.67% and sensitivity and specificity of 90% and 93.33% respectively.

MATERIALS AND METHOD

The objective of this paper is to develop a computer-based approach to detect the different diabetic retinopathy stages using fundus images. A simple and user friendly interface is also necessary as the user might not be proficient in programming code. The overall objective of this paper is to create an automated program to quickly process a large number of fundus images from mass screening of diabetic retinopathy accurately. Diabetic retinopathy in non-proliferative diabetes retinopathy or proliferative diabetes retinopathy stages can lead to visual impairment or even blindness. Hence, this system could assist ophthalmologists to improve their productivity, efficiency as well as cost effective, in detecting the different stages of diabetic retinopathy and identify patients for early treatment to prevent or delay visual loss. This paper uses the classification system of Normal, Mild and Higher stages to classify the NPDR and PDR as shown in Fig 1.5. The first approach to this project is a background study of fundus images to determine the features to extract and use. The fundus images are also analyzed to recognize their similarity and differences. Familiarizing with MATLAB Image Processing Toolbox is also important prior to the commencing of features extraction. After getting the values of the features from the images, Artificial Neural Network (ANN) would be studied and applied for automatic detection. The results would be tested for accuracy and troubleshooting or fine-tuning of the codes might be required. Lastly, a Graphical User Interface (GUI) to access the automated program would be developed and all the findings and results would be recorded and documented.

Features Extraction: Figure 6 shows the overall block diagram and Architecture of the whole program. The fundus images are converted to either green component or grayscale for features extraction of texture analysis.

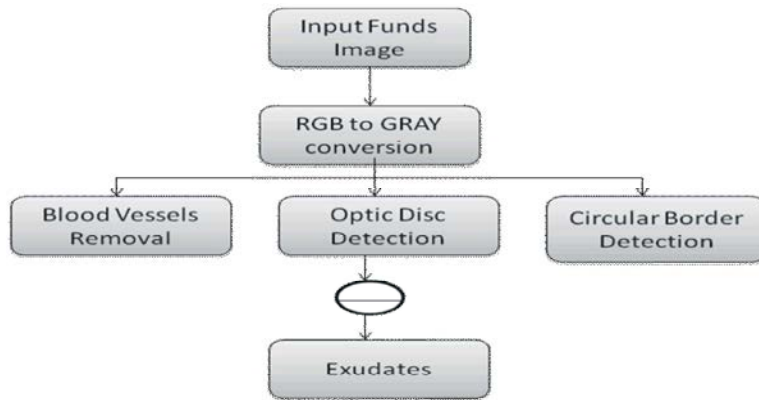


Fig. 6: Block Diagram of Overall Architecture of diabetic retinopathy

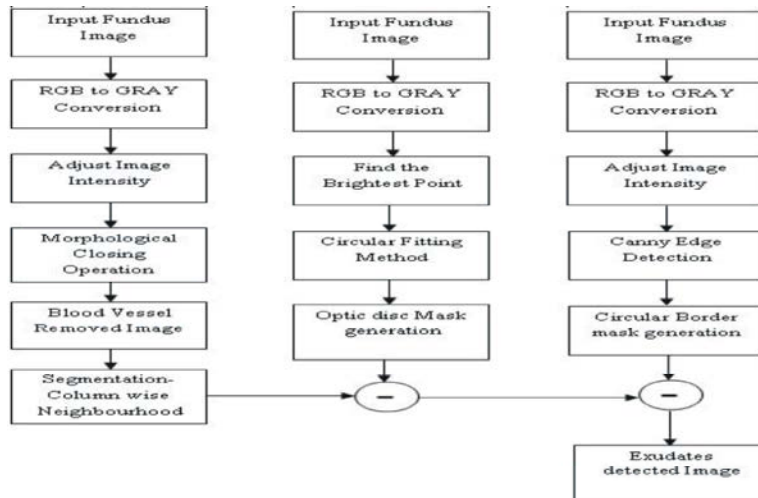


Fig. 7: Block Diagram of Overall System of diabetic retinopathy

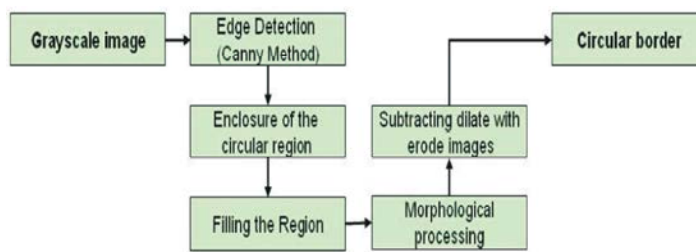


Fig. 8: Block Diagram for Border Formation - Method 1

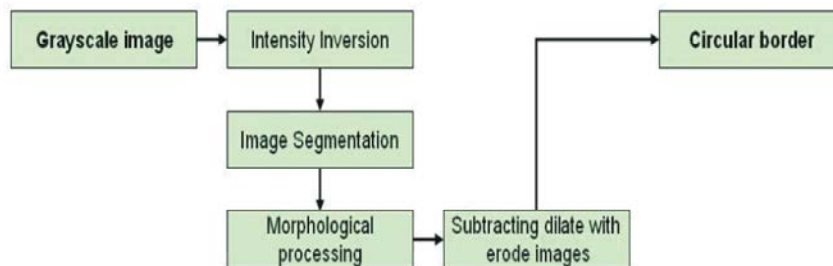


Fig. 9: Block Diagram for Border Formation - Method 2



Fig. 10: Circular border obtained using either method

The normalized features' values are then fed into Morphological closing operations, blood vessels will be removed. using Canny edge detection, the edges of the internal part of fundus image will be detected. The column wise neighbourhood operations are performed using matlab syntax Colfilt. Integration of all three operations results in detection of exudates in input fundus image.

Border Formation: There are two methods in detecting the circular border of the image. Both methods are essential as each method could not work for a few of the images due to their intensity contrast. Deploying both methods allows the detection of all the images. Border formation is to clean off the noisy edges and is also used during Exudates and Micro aneurysms detection.

Border Formation Method 1: Grayscale image instead of the green channel is used as it is more efficient in border detection. The first method uses canny method to detect the edges before enclosing the circular region with a top and bottom bar. Function "imfill" is then applied to fill the region. The circular border is obtained after subtracting the dilated image with the eroded image is shown in fig 8.

Border Formation Method 2: Method 2 (Shown in fig 9) is activated when a noisy image is obtained instead of a circular border. This method inverts the intensity of the image first before image segmentation is applied with the function "im2bw". The circular region is filled as a result and the circular border is obtained after subtracting the dilated image with the eroded image is shown in fig 10.

As the optical disk is made up of a group of bright spots, it is not suitable to use loops and locate the largest value. This would only point to one spot and most likely

to be on the side of the optical disk. The mask required to cover the optical disk would be inefficient as it would be much larger and covers more details. Mask creation is used in the detection of blood vessels, exudates and micro aneurysms. Grayscale image instead of the green channel is used as it is more efficient in the detection. The above lines would first find the max value for each of the 720 columns of the image before locating the largest value. The coordinates (row and column) of all brightest point(s) are then determined and the median is taken if there is more than one point. After locating the optical

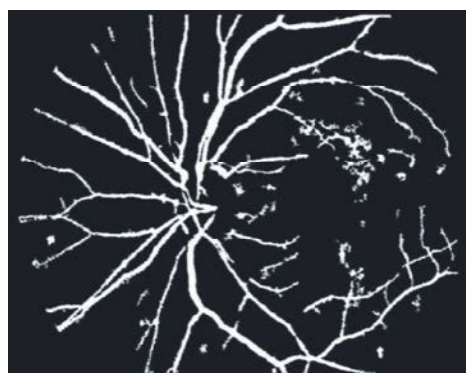


Fig. 11: Comparing blood vessels images obtained

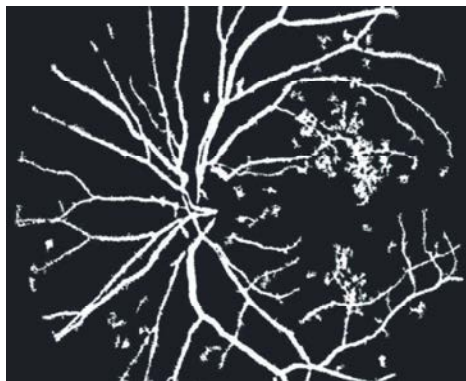


Fig. 12: Blood vessels image after apply AND logic

disk, a mask needs to be created. A simple square mask created using loops would be easy but this would result in error when the optical disk is close to the border of the image. The above lines are used instead to generate the circular mask.

$$R^2=(x-h)^2+(y-k)^2$$

The function “meshgrid” is to generate X and Y matrices while the next line that creates the mask is the equation for drawing circle. H and K are the coordinates (row and column) and R as the Radius.

Experimental Procedure-and Logic: Two methods of detecting the blood vessels are used. Both methods would generally detect different locations of the images like exudates as blood vessels; hence by computing their similarity, the non blood vessels area could be filtered is shown in fig 11.

AND logic is applied to mark out the similar pixels of the two images. The output pixel is registered as binary 1 (white) when the both images’ pixels are binary 1 (white). The obtained image would be a clearer blood vessels image shown in fig 12.

RESULTS

The area of the blood vessels is obtained by using two loops to count the number of pixels with binary 1 (white) in the final blood vessel image shown in fig 13.

ANOVA Test Results: Table 1 shows the values of all the subjects are input into Analysis of Variance to test the hypotheses between the groups.

Masking at the optical disk is essential for AND logic as some of blood vessels there are lost after applying adaptive histogram equalization and image segmentation. It is noted that some of the images have noise within the mask area and detect as blood vessels but it is still trivial to affect the overall value. The higher stage of the diabetic retinopathy is known to have more blood vessels due to damages and growth and the overall obtained result matched it. However, the large standard deviation value might affect the output result of the ANN.

Exudates Detection: Exudates appeared as bright yellow-white deposits on the retina due to the leakage of blood from abnormal vessels. Their shape and size will

Table 1: ANOVA test result for Blood Vessels

Feature	Higher	Mild	Normal	P-value
Mean Blood Vessels Area	43412	39097	36161	0.0081
± Std dev	± 11044	± 9374	± 6987	

Total subjects - 98

Std dev - Standard deviation, P-value - The probability of the result.

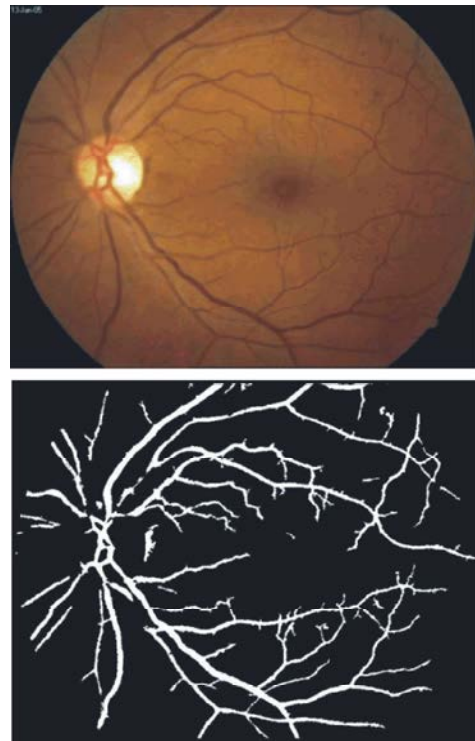


Fig. 13: Fundus image (Left) with its blood vessels image (Right)

vary with different retinopathy stages. The grayscale image is first preprocessed for uniformity before the morphological image processing is applied to remove the blood vessels and identify the exudates region. The exudates are detected after removing the border, optical disk and non-exudates area.

Figure 14 discusses in greater detail of the extraction of the exudates. The fundus image is first preprocessed to standardize its size to 576x720 and the intensity of the grayscale image is then adjusted shown in fig 15 and 16.

Morphological closing which consisted of dilate followed by erode is applied to removed the blood vessels. The dilate function expands the exudates area while erode function removes the blood vessels. The image (Figure 17) is then converted to double-precision value for function “colfilt” to mark

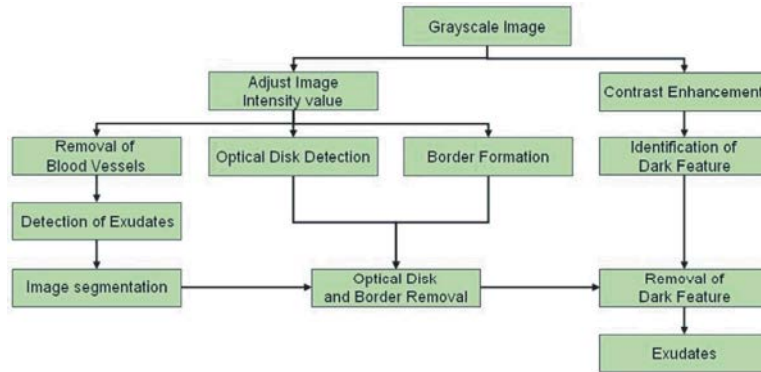


Fig. 14: Block Diagram for Exudates Detection



Fig. 15: Original fundus image



Fig. 18: Mask for the Optical Disk

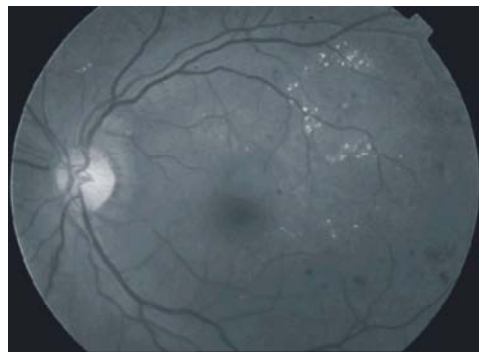


Fig. 16: Intensity adjusted grayscale image



Fig. 19: Image with Optical Disk removed



Fig. 17: Image after Morphological Closing

the exudates region before converted back as shown in (Figure 18). This image is converted back to binary using the function “im2bw” with a threshold value to filter out the exudates.

The location of the optical disk is detected by the brightest point(s) on the grayscale image. It is usually the maximum value and a circular mask is then created to cover it.

The regions of the exudates (Shown in figure 20) obtained after the removal of the circular border. Morphological closing is then applied to the image.

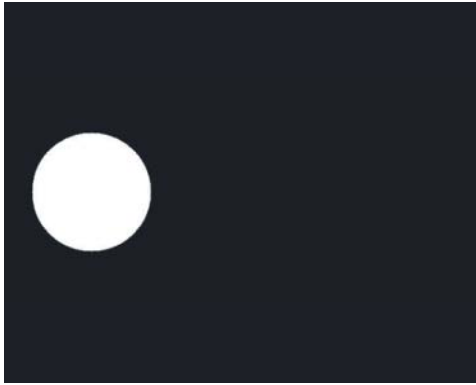


Fig. 20: Regions of exudates

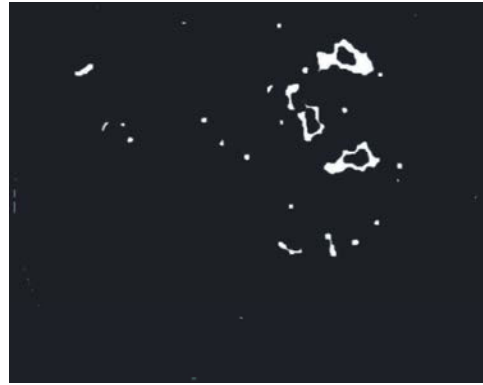


Fig. 23: Exudates after performing (represented as white) 'AND' logic



Fig. 21: Image after Morphological closing



Fig. 24: Expanded exudates regions



Fig. 22: Image with Dark features



Fig. 25: Dark features represented as after Morphological closing white

The dilate function is to fill the exudates while erode function is to expand their sizes shown in fig 21.

Non-exudates (dark features) are extracted from the grayscale image using function "im2bw" and are represented as binary 1 (white) after intensity inversion. AND logic (to be further discussed in the section 4.3.3) is then applied to the images (Figure 22 and Figure 23) to detect the exudates (Figure 24).

Experimental Procedure-and Logic: AND logic is used to remove noise for the detection of exudates. Regions with exudates are marked out after applying column filter but this includes non-exudates such as hemorrhages and has to be removed as noise.

By removing the non-exudates from the detected regions, the exudates can be determined.

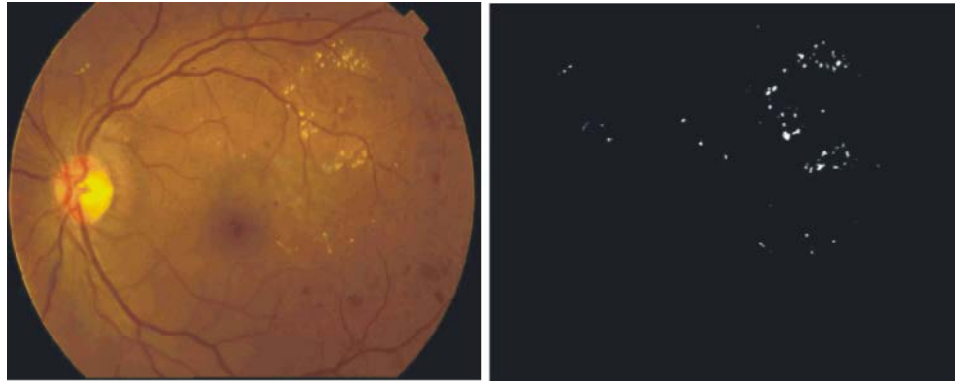


Fig. 26: Fundus image (Left) with its exudates image (Right)

Table 2: ANOVA test result for Exudates

Feature	Higher	Mild	Normal	P-value
Mean Exudates	919.68	58.25	6.09	<0.0001
Area \pm Std dev	\pm 714.98	\pm 108.09	\pm 11.88	

Image segmentation is applied to the grayscale image to extract the bright spots for comparison. These areas (bright features) are represented by binary 0 (black) while the non-exudates (dark features) are represented as binary 1 (white) as shown in Figure 25. By applying AND logic to Figure 24 and Figure 25 the non-exudates regions are set to set to binary 0 (black) and removed when the pixels for both images are binary 1 (white). As a result, the exudates area is obtained is shown in fig 26.

ANOVA Test Results: Table 2 shows the values of all the subjects are input into Analysis of Variance to test the hypotheses between the groups

DISCUSSION

The higher stage of the diabetic retinopathy would have more exudates due to damages or leakages of the blood vessels and the overall obtained result matched it. The mask detection of the optical disk could take the exudates coordinates instead when they are much brighter or close together and forms a larger area than the optical disk. Some of the images had exudates area masked as a result; however it is trivial to affect the overall value as those images generally had a large area of exudates.

CONCLUSION

Biomedical image processing requires an integrated knowledge in mathematics, statistics, programming and biology. Based on the results of the

classifier, this paper has a Accuracy 94%, sensitivity of 80% and a specificity of 20%. It is able to achieve a fairly accurate classification for mild and higher stages but not for normal class resulting in a possible high false alarm. This might be improved by fine tuning the threshold values used on the images and more images could be used to improve the overall system. For this paper, we had learnt various techniques of image processing and was able to extract the features, namely blood vessels, exudates, micro aneurysms and texture properties (homogeneity and entropy) from the fundus images.

REFERENCES

1. Abdelrahim Nasser Alan Murray, 2002. "Fractal Analysis in the Detection of Colonic Cancer Images," IEEE Transactions on Information Technology in Biomedicine, 6(1): 54-58.
2. Aminesh Naseri, Ali. Pouyan and Nader Kavian, 2012. "Automatic Detection of Retina Layers using Texture Analysis," International Journal of Computer Applications, 46(1): 29-33.
3. Barry R. Masters, 2004. "Fractal Analysis of the Vascular Tree in the Human Retina," Annu. Rev. IEEE Transactions on Biomedical Engineering, 6: 427-452.
4. Hatanaka, Y., T. Yamamoto and H. Fujita, 2010. "Automatic measurement of vertical cup-to disc ratio on retinal fundus images," in Proc. International Conference Meddical Biometrics, 10: 64-72.
5. Jian Li, Qian Du and Caixin Sun, 2009. "An improved box-counting method for image fractal dimension estimation," IEEE Transactions on Pattern Recognition, 42: 2460-2469.

6. Kevin P. Noronha and Sulatha V. Bhandary, 2013. "Automated classification of glaucoma stages using higher order cumulant features," IEEE Transactions on Biomedical Signal Processing and Control.
7. Malaya Kumar Nath and Samarendra Dandapat, 2012. "Differential entropy in wavelet sub-band for assessment of glaucoma," International Journal Systems and Technology, 22(3): 161-165.
8. Muthu, M., Rama Krishnan, Oliver Faust, 2013. "Automated glaucoma detection using hybrid feature extraction in retinal fundus images," Journal of Mechanics in Medicine and Biology, 13: 1350011-1-1350011-21,
9. Radim Kolar and Jiri Jan, 2008. "Detection of Glaucomatous Eye via Color Fundus Images Using Fractal Dimensions," Journal of Radio engineering, 17: 109-114.
10. Rajendra, U. Acharya and Chua Kuang Chua, 2011. "Automated Diagnosis of Glaucoma Using Texture and Higher order Spectra Features," IEEE Transactions on Information Technology and Biomedicine, 15(3): 449-455.
11. Rudiger Bock and Georg Michelson, 2010. "Glaucoma risk index: Automated glaucoma detection from color fundus images," Journal of Medical Image Analysis, 14: 471-481.
12. Shun-Chen Cheng, 2003. "A Novel Approach to Diagnose Based on the Fractal Characteristics of Retinal Images," IEEE Transactions on Information Technology and Biomedicine, 7(3): 163-170.
13. Stefan Talu and Stefano Giovanzana, 2011. "Fractal and Multifractal analysis of human retinal vascular network: a review," Human and Veterinary Medicine and International Journal of the Bioflux Society, 3(3): 205-212.